Jet Stream Dynamics, Hydroclimate, and Fire in California: 1600 CE to Present

Eugene Wahl[1], Eduardo Zorita[2], Valerie Trouet[3], Alan Taylor[4]

[1]NOAA, [2]Helmholz-Zentrum Geesthacht, [3]University of Arizona, USA, [4]The Pennsylvania State University

Submitted to Proceedings of the National Academy of Sciences of the United States of America

Moisture delivery in California is largely regulated by the strength and position of winter high-altitude winds, the North Pacific Jet (NPJ), which influences regional hydroclimate and forest fire during the following warm season. We use climate model simulations and paleoclimate data to reconstruct winter NPJ characteristics back to the 16th century, to identify the influence of NPJ behavior on moisture and forest fire extremes in California prior to and during the more recent period of fire suppression. Maximum zonal NPJ velocity is lower, northward shifted, and has a larger latitudinal spread during pre-suppression dry and high-fire extremes. Conversely, maximum zonal NPJ is higher, southward shifted, and has narrower latitudinal spread during wet and low-fire extremes. These NPJ, precipitation, and fire associations hold across pre-20th century socio-ecological fire regimes including Native American burning, post-contact disruption and native population decline, and intensification of forest use during the later 19th century. Precipitation extremes and NPJ behavior remain closely linked in the 20th-21st century, but fire extremes become uncoupled due to fire suppression after 1900. Simulated future conditions in California include more wet season moisture as rain and less snow, a longer fire season, and higher temperatures, leading to drier fire season conditions independent of 21st century precipitation changes. Assuming continuation of current fire management practices, thermodynamic warming is expected to override the dynamical influence of the NPJ on climate-fire relationships controlling fire extremes in California. Recent widespread fires in California in association with wet NPJ extremes may be early evidence of this change.

Jet Stream | Precipitation | Fire | California | Paleoclimatology

The severe drought experienced in California (CA) from 2012-2015 CE (CE is omitted hereafter) impacted its economy and environment, reducing water availability for urban and agriculture consumers along with hydroelectric power generation (1), and increasing tree mortality and wildfire risk (2). High precipitation events in the wet seasons of 2016 and 2017 relieved immediate effects of this four-year drought, but their magnitude highlights the problematic nature of precipitation extremes and the need to simultaneously cope with the effects of both severe drought and flooding (3). The extreme nature of the polarities – exemplified by a 500-year record low Sierra Nevada snowpack in 2015 (4) followed by threats to major dam integrity and widespread flooding (5) along with the 506k acres burned in 2017 (6), which caused the greatest loss of life and economic value in CA history – raises questions about the contribution of anthropogenic climate change to these events and its future impacts. Extreme drought in CA occurs when low winter precipitation coincides with unusually high temperatures and these conditions have become more frequent with rising temperatures in recent decades (7). In extreme warm/wet years such as 2017, with very deep Sierra Nevada snowpack and abundant precipitation, intense rainfall can result in large floods and power outages (8). High spring and summer temperatures rapidly desiccate abundant fuels produced by the high precipitation, and when combined with high winds can greatly increase area burned and loss of life in wildfires that are difficult to control, as exemplified by the tragic Tubbs Fire in October 2017, the Thomas Fire in December 2017, and the Mendocino fire in 2018 (9).

Most climate simulations agree that CA will warm in the 21st century (10), but the projections for future precipitation patterns – strongly linked to North Pacific Jet (NPJ) dynamics that regulate moisture delivery from the Pacific Ocean – are less unanimous. During the 2012-2015 drought in CA, the North Pacific blocking ridge was unusually persistent ("the ridiculously resilient ridge") and formed a dipole with an equally persistent trough over east-central to far northeastern North America (11) (See SI Appendix, Fig. S1); this dipole pattern has been linked to a warming North Pacific Ocean (12). The association between North Pacific blocking and CA drought is also reflected in increased CA fire risk (13) and annual area burned (14) and is consistent with paleoclimate reconstructions of high sea level pressure for extreme dry years in CA (15). During the winter of 2015-2016, the blocking ridge was significantly reduced in strength, and its center in western North America had shifted northeastward into Canada (See SI Appendix, Fig. S1). By the winter of 2016-2017, a deep low pressure anomaly covered much of the mid- to high-latitude North Pacific (See SI Appendix, Fig. S1), allowing NPJ-driven Pacific storm tracks to deliver large amounts of moisture into CA, notably in the form of atmospheric rivers (16).

With drought, large precipitation events (8), and CA fire weather projected to become more extreme with anthropogenic climate changes (17), it is essential to improve our understanding of North Pacific circulation as a driver of extreme events to

Significance

North Pacific jet stream (NPJ) behavior strongly affects cool-season moisture delivery in California, and it is an important predictor of summer fire conditions. New reconstructions of the NPJ before modern fire suppression began in the early 20th century identify the relationships between precipitation and fire extremes and NPJ characteristics. After fire suppression, the relationship between the NPJ and precipitation extremes is unchanged, but the NPJ-fire extremes relationship breaks down. By 2070-2100, simulations with high CO_2 forcing show higher temperatures, reduced snowpack, and drier summers whether overall precipitation is enhanced or reduced, thereby overriding historical dynamic NPJ precursor conditions and increasing fire potential due to thermodynamic warming. Recent California fires during wet NPJ extremes may be early evidence of this change.

Reserved for Publication Footnotes

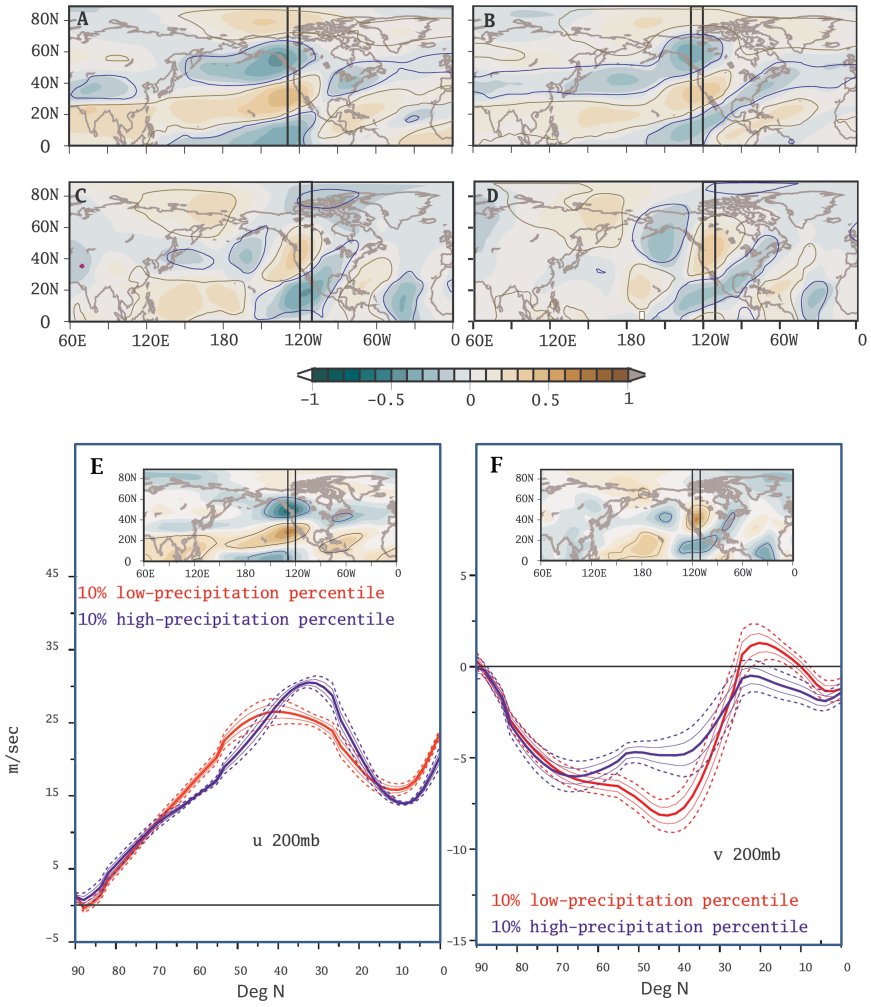

Fig. 1. Linkages between winter North Pacific Jet Stream (NPJ) winds and California precipitation and fire activity. (a-d) Correlation maps between reconstructed Sierra Nevada precipitation (23) or fire activity (24) and zonal (*u*) and meridional (*v*) components of the winter (December$_{t-1}$-February$_t$) 200 hPa wind reconstructed from MPI-ESM-P model: (a) precipitation and *u*-component, (b) fire activity (inverted) and *u*-component, (c) precipitation and *v*-component, (d) fire activity (inverted) and *v*-component; rectangles show longitudinal windows where correlations between the wind components and precipitation and fire activity are jointly highest (120W-130W for *u*-component, 110W-120W for *v*-component), used for analysis of maximum winds; time periods are 1571-1903 for precipitation (to earliest year of NPJ data) and 1600-1903 for fire activity (to earliest year of fire data). (e-f) Latitudinal profiles of: (e) 200 hPa *u*-wind velocity, averaged between 120W-130W, and (f) 200 hPa *v*-wind velocity, averaged between 110W-120W, for the 10% driest (red) and 10% wettest (blue) winters in California during 1904-2013, according to the 20th Century Reanalysis (20CR v2) (26); thick solid lines indicate mean values at each latitude for each set of winters; thin solid (dashed) lines indicate +- 1 (+- 2) times the sample-estimated standard error of the mean; insets show correlations maps for 20CR v2 precipitation and *u*- and *v*-components, as in (a) and (c). Contour lines in correlation plots indicate $p < 0.05$ significance levels (brown-positive, blue-negative), corrected for autocorrelation for each grid cell time series (51).

anticipate future socio-environmental impacts. Here, we present a 400-year reconstruction of NPJ variability to understand its impact on historical CA precipitation and wildfire since 1600. For this analysis, we use an off-line paleo data-assimilation scheme (18) to reconstruct atmospheric circulation at 200 hPa geopotential height – an atmospheric level typically used to characterize the behavior of the NPJ – during Northern Hemisphere winter (December$_{t-1}$-February$_t$), the months CA receives more than half its annual precipitation (19). The reconstruction spans the period 1571-1977, and focuses on developing reconstruction skill for the sectors most relevant for CA precipitation, the northeastern Pacific Ocean and coastal western North America. The primary Earth System Model (ESM) we employ is the Max Plank Institute MPI-ESM-P (see Methods and SI Appendix for details of the reconstruction and criteria for ESM selection). Our reconstruction is the first of its kind for the upper troposphere and represents an important extension for this region in last-millennium paleoclimatology, which seeks to develop spatially-explicit, annually-resolved reconstructions of precipitation and circulation fields (cf. 18, 20-22).

We couple the NPJ reconstruction with a separate reconstruction of Sierra Nevada precipitation (23) and an index of Sierra Nevada fire extent (24), to identify NPJ influence on extreme dry (wet) and high (low) fire years in CA. The fire index measures fire activity as recorded in tree rings and historical fire records across the entire length of the Sierra Nevada and represents fire extent at a regional scale appropriate for comparison with synoptic-scale NPJ reconstructions; our evaluation begins in 1600 (See SI Appendix, Fig. S2 and Methods). Four fire regimes linked to distinct socio-ecological conditions are evident in the fire record (24), and we stratify our results and analyses across these regimes. The regimes include: pre-contact Native American subsistence burning (1600-1775), post-contact disruption and native American depopulation (1776-1865), intensification of Euro-American forest use in the late 19th century (1866-1903), and the 1904-present period of modern fire suppression (24). An additional regime sub-division was added at 1977, to isolate the later part of the 20th and early 21st centuries when there were state changes in the northern Pacific Ocean (25), temperature, and increased fire extent (17, 19, 24). The novel combination of high-resolution paleoclimate and paleofire activity permits characterization of the mechanistic relationship between NPJ behavior, moisture delivery, and fire extent over a period nearly four times longer than the instrumental record, including a spectrum of human modulated fire regimes.

We first characterize the relationship between CA precipitation and 200 hPa wind in the Twentieth Century Reanalysis (20CR v2), a fully independent instrumental data and model-based estimate of daily atmospheric circulation (26), and compare it to our reconstruction. The spatial pattern of correlation between CA winter precipitation and the winter 200 hPa wind field for the reanalysis (1904-2013; Fig. 1e-f, inserts) is very similar to the spatial correlation between both CA precipitation *and* fire activity and the winter 200 hPa wind field for the reconstruction

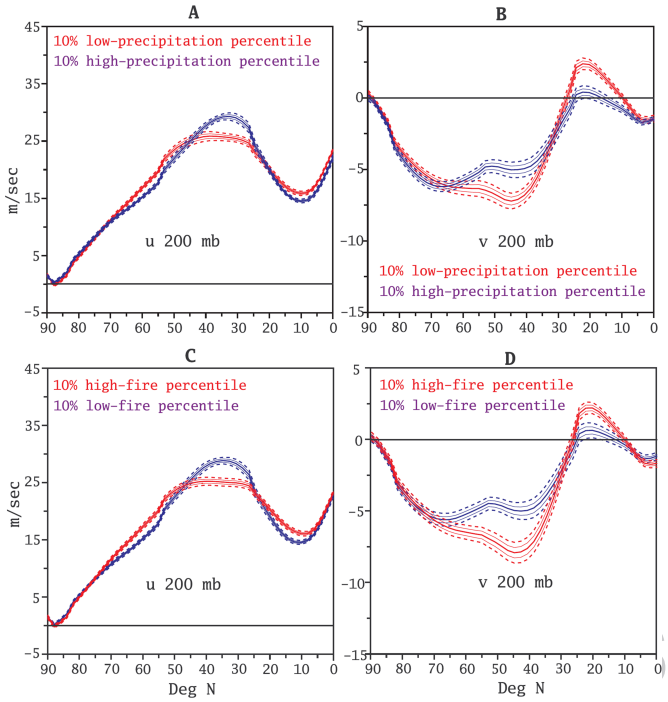

Fig. 2. Latitudinal profiles of reconstructed winter North Pacific Jet Stream wind velocity for extreme precipitation and fire years in California - prior to modern fire suppression. (a) mean 200 hPa *u*-wind velocity for the 10% driest (red) and 10% wettest (blue) winters according to reconstructed Sierra Nevada precipitation (23); (b) as (a) but for the mean 200 hPa *v*-wind; (c) mean 200 hPa *u*-wind for the 10% years with most (red) and 10% years with least (blue) Sierra Nevada fire activity (24); (d) as (c) but for the mean 200 hPa *v*-wind; thick solid lines indicate mean values at each latitude for each set of winters; thin solid (dashed) lines indicate +-1 (+- 2) times the sample-estimated standard error of the mean. Jet stream winds are averaged between 120W-130W for the *u*-component and 110W-120W for the *v*-component; time periods are 1571-1903 for precipitation extremes (to earliest year of NPJ data) and 1600-1903 for fire extremes (to earliest year of fire data).

(Fig. 1a-d). Low precipitation extremes in the reanalysis (Fig. 1e, red curve) and reconstructed pre-20th century extremes for both dry and high-fire conditions (defined as ≤ 10% and ≥ 90% of their distributions, respectively) (Fig. 2a,c, red curves) are strongly associated with a weakening, northward shifted extent, and wider latitudinal spread of maximum velocity, centered at ~39-41° N, for the NPJ zonal (*u*) component (NPJ_u) in the northeastern Pacific and far western North America. Conversely, extreme wet and low-fire conditions (defined as ≥ 90% and ≤ 10% of their distributions, respectively) are strongly associated with a strengthening, southward shifted extent, and narrower latitudinal spread of NPJ_u maximum velocity, centered at ~33-34° N (Figs. 1e and 2a,c, blue curves), which increases precipitation from northern Pacific storm track activity and moist tropical air flow into CA. The NPJ meridional (*v*) component (NPJ_v) is stronger and more negative in the study region during dry extremes (Figs. 1f and 2b, red curves), corresponding to more northerly flow and a characteristic blocking high pressure ridge (See SI Appendix, Fig. S1); the same NPJ_v pattern is evident for high-fire years (Fig. 2d, red curve). The generally close correspondence of the reanalysis and reconstruction precipitation results over the common 1904-1977 period (Figs. 3a-b, 4d,h) serves as additional validation of the NPJ reconstruction (See SI Appendix, *Additional Methodological Detail* and Fig. S5d), along with the Sierra Nevada precipitation and fire data used to evaluate moisture and fire extremes relationships for the paleo-reconstruction period evaluated here.

The relationship of the NPJ to precipitation and fire extremes (Figs. 4 and 5) remains largely constant over the reconstruction period despite the four distinct regimes of fire extent related to changes in human activity. Separation of the precipitation and fire extremes in terms of NPJ_u maximum velocity is relatively weaker during the 1904-1977 period with fire suppression compared to earlier fire regimes (Figs. 4d and 5d), and is most evident for the extreme dry case (Fig. 4d). The maximum of NPJ_v exhibits a southward shift coupled with a relatively steeper latitudinal gradient over CA for the extreme wet case during the 1600-1775 and 1904-1977 regimes (Fig. 4e,h). This feature indicates that the wet and low-fire extreme years were more distinct during these two regimes than during the two intervening ones, 1776-1903, and that the difference was primarily evident in NPJ_v.

The effect of modern fire suppression management on the NPJ-fire extremes relationship since 1904 is even more evident in the reanalysis data (Fig. 3e-h). As with the reconstruction, there is statistically meaningful separation in NPJ_u maximum velocity between high- and low-fire extremes during the 1904-1977 period (Figs. 5d and 3e), but there is much less separation than for the corresponding extreme precipitation case (Fig. 3a). More notably, NPJ_u maximum velocity for the extreme low-fire case is reduced and shifted to northern CA at ~39° N and the flatness of the velocity profile for the high-fire case extends to northern Mexico (Fig. 3e). During 1978-2013 there is no difference in NPJ_u between the high- and low-fire cases (Fig. 3g), in clear contrast to the differences for NPJ_u for the extreme precipitation cases (Fig. 3c), notwithstanding enhancement of estimated uncertainties for the 1978-2013 period due to reduced sample size. Similarly, there is no difference in NPJ_v between the high- and low-fire cases throughout the post-1904 period (Fig. 3f,h), again in clear contrast to the 1904-1977 extreme precipitation cases (Fig. 3b), but with less contrast to the 1978-2013 precipitation extremes (Fig. 3d). The steepness and amplitude of the latitudinal gradient of NPJ_v in the CA region continues to be greater for the high-fire versus low-fire cases during this time (Fig. 3f,h). Notably, however, both cases exhibit greater range in NPJ_v amplitude, and the gradient steepness for the low-fire case is stronger, than in the corresponding reconstruction results (Fig. 5h) and the reanalysis extreme precipitation case during 1904-1977 (Fig. 3b). The erosion of 20th century NPJ-fire relationships and then the full uncoupling of fire from NPJ_u after 1977 documents recent amplification of fire regime regulation by humans.

Our results complement and extend two recent studies that focus on wet-season cyclonic storm track position (strongly associated with the NPJ) in the Pacific Northwest region of the United States. The first (27) presents index reconstructions of storm track latitudes across a set of longitudinal transects for the period 1693-1995; the second (28) evaluates the recent period 1980-2014 and relates storm track position to forest growth and fire activity in western North America. The Pacific Northwest is the region of typical wet-season storm entry into mid-latitude western North America (28, 29), and subtle differences in the central storm track latitude there can have a large influence on regional hydroclimate (27). In contrast, much of CA lies south of the general northeastern Pacific storm track and relatively large, transient latitudinal excursions of the storm track center are strongly associated with winter moisture delivery (29), as noted here (Figs. 1e, 2a,c, 3a,c, and 4a-d). Our reconstructions extend examination of storm track-related NPJ behavior along the Pacific Coast a century further into the past, and, importantly, provide full, physically consistent, reconstruction of the 200 hPa atmospheric circulation for a large portion of the northeastern Pacific region and adjacent North America over an even longer period, to 1571 (see Methods, *Data Availability*). Additionally, we couple this longer circulation record with corresponding precipitation and fire activity records in the Sierra Nevada, including

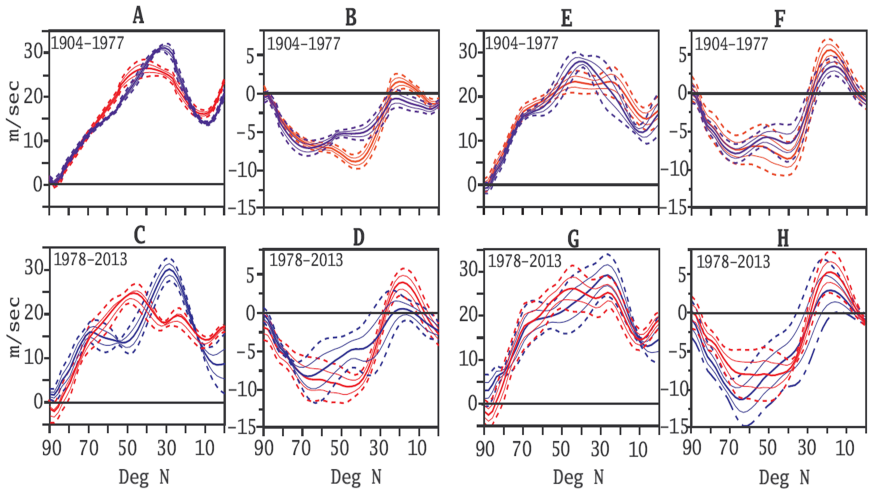

Fig. 3. North Pacific Jet Stream *u*- and *v*-wind Behavior Related to Precipitation (a-d) and Fire (e-h) Extremes over Social Usage Regime Sub-Divisions, 1904-2013. As Figure 1e-f from 20th Century Reanalysis (20CR v2) data (26); additionally including fire regime sub-division at 1977 described in text.

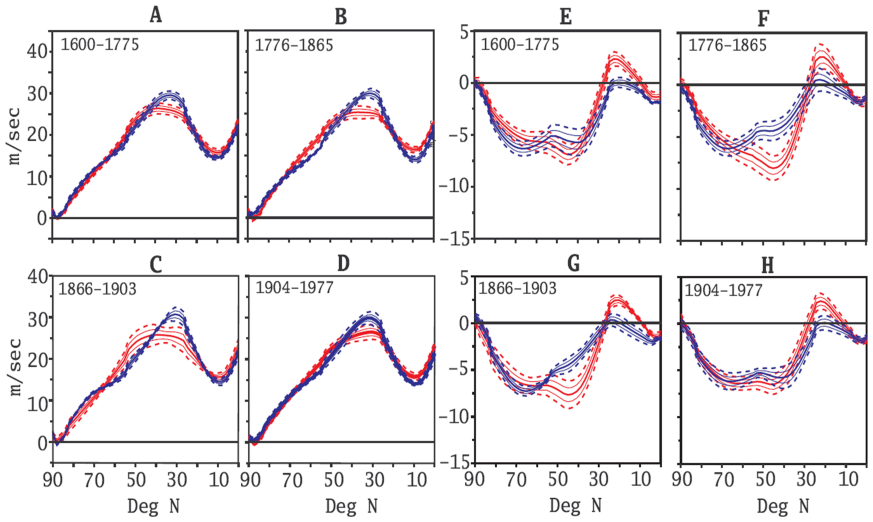

Fig. 4. North Pacific Jet Stream *u*- and *v*-wind Behavior Related to Precipitation Extremes over Social Usage Regimes, 1600-1977. As Figure 2a-b from reconstructions, but for fire usage regime periods defined in (24).

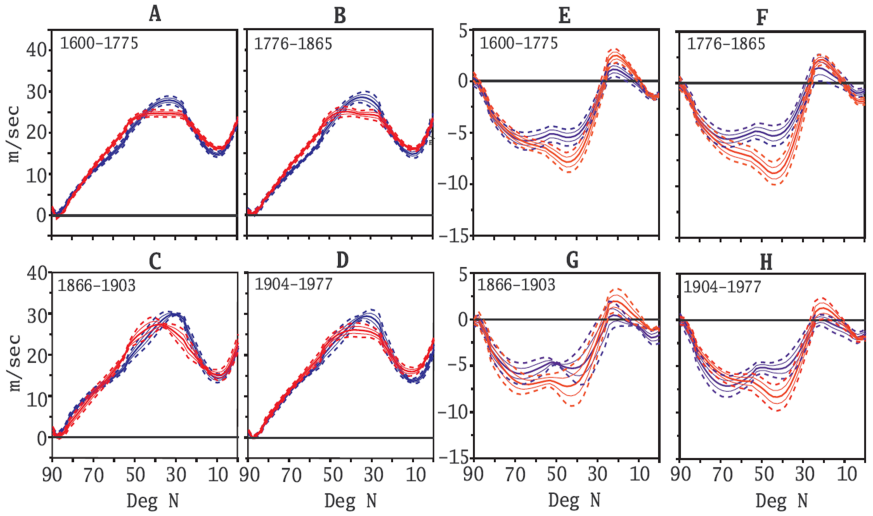

Fig. 5. North Pacific Jet Stream *u*- and *v*-wind Behavior Related to Fire Extremes over Social Usage Regimes, 1600-1977. As Figure 2c-d from reconstructions, but for fire usage regime periods defined in (24).

socially-driven changes in fire activity, providing an opportunity to evaluate the combined influences of paleo-circulation, paleo-precipitation, and paleo-fire to inform understanding of drivers of precipitation and fire in CA forests since 1600.

Climate models generally agree that temperatures are projected to increase in the future (10) and this, in association with enhanced vapor pressure deficits that are already occurring (30), will increase warm-season fire risk (17). The models have less convergence regarding antecedent cool-season precipitation (31). While most of the CMIP5 models project at least a small increase in winter precipitation over most of CA under the RCP8.5 scenario, a minority do not (31); this reduced convergence is likely due to the location of CA in the transition zone between simulated mid-latitude increases and subtropical decreases in precipitation (31) and to regional heterogeneity in the projected future shift of the mid-latitude jets (32). The MPI-ESM-P model we utilize for paleo- and modern-period analysis is in the model majority, and simulates winter NPJ conditions under the RCP8.5 scenario that are most consistent with the pre-20th century high precipitation/low fire state (See SI Appendix, Fig S3). In conjunction with increasing temperatures, however, more of this winter precipitation would occur as rain relative to snow (33) (See SI Appendix, Fig. S4d), reducing snowpack duration (34) and, along with enhanced vapor pressure deficits (30), would lead to earlier warm-season forest drying compared to the same NPJ conditions prior to modern fire suppression. Thus, by the later 21st century, the relationship of fire extremes and winter climate precursor conditions in CA montane forests could potentially have no ecological parallel compared to winter conditions prior to modern fire suppression. In terms of climate physics, while winter precursor conditions for CA wildfire were strongly dynamically-driven by NPJ activity prior to modern fire suppression (Figs. 2c-d, 5a-c,e-g), potential future increases in temperature and corresponding reductions in the snow-to-rain ratio would result in a shift to fire conditions (separate from suppression efforts per se) that are more thermodynamically controlled, both in terms of the winter precursor conditions and summer "fire weather" itself (35). The recent widespread fires in CA's forests (9) may be early evidence of this change; in our record, the pre-suppression period 1600-1903 does not contain a single case of a high-precipitation year coupled with a high-fire year, as occurred in 2017.

If it occurs, such a fundamental reorganization of climate controls will not only likely promote the incidence of "megafires" (36) in fuel-rich forests that have experienced a century of fire suppression (37), but also entrain second- and third-order effects that alter species distributions, forest composition, and ecosystem function (i.e., productivity, carbon and water cycling) (38). Our work provides a new, critical multi-century perspective on the physical drivers of climate that could reorganize CA forest ecosystems and their disturbances. It also provides a stronger foundation and a longer-term perspective for evaluating regional natural hazards and economic risk to CA under the RCP8.5 scenario in one of the world's largest economies.

Methods

Atmospheric Circulation Field Reconstruction

We used an analog assimilation method similar to that applied in other studies (18, 39-42) to reconstruct three-dimensional fields of the atmospheric circulation, based on a combination of state-of-the-art climate model output [MPI-ESM-P (43), NCAR-CCSM4 (44), and GISS-E2R (45) last millennium transient-forcing simulations, see SI Appendix, *Earth System Model Selection and Evaluation*] with three gridded paleoclimate reconstructions. The reconstruction predictors include tree ring-based reconstructions of June-August$_t$ (JJA) soil moisture (the North American Drought Atlas, or NADA) (46), water-year$_t$ (WY, October$_{t-1}$ through September$_t$) precipitation (15, 20), and February-March$_t$ (FM) near-surface air temperature (47) over portions of western and southwestern North America. For a given calendar year *t*, the predictor fields are compared to the simulated seasonal mean fields of the same variables through the length of the climate simulations; the years for which the simulated seasonal fields are most similar to the gridded reconstructions are considered the 'analog years' and the atmospheric circulation (the predictand) of the corresponding winter (December$_{t-1}$-February$_t$, DJF) season is selected to form the model-based reconstruction. To define the most similar analogs, the three climate variables were merged into a single vector for each year after they were regridded to a common 2.5 x 2.5 longitude/latitude grid, and then normalized so that each variable had the same weight in the definition of similarity to the simulation output.

The physical basis for this strategy is the strong relationship between the winter atmospheric circulation over the northeastern Pacific-western North American sector and these variables. Winter temperatures are directly influenced by this circulation via air mass advection and the two hydrological variables also strongly depend on the moisture delivery from the Pacific onto land that occurs during the winter season. As noted, CA receives more than half its annual precipitation during winter (19), and the NADA has been shown to be strongly related to antecedent winter moisture delivery south and west of a line connecting the northwestern United States to northeastern Mexico (48), which is the regional portion utilized here. Employing the analog method, the global three-dimensional field of the atmospheric circulation can in principle be reconstructed, although the actual reconstruction skill will be spatially heterogeneous and generally higher in the regions where the atmospheric circulation most strongly influences the predictors (See SI Appendix, Fig. S5). We note the similarity of this reconstruction process to the "Proxy Surrogate Reconstruction" method outlined in (49).

We extracted 200 hPa zonal (*u*) and meridional (*v*) wind components from the reconstructed circulation fields for analysis of winter NPJ conditions. We analyzed the latitudinal position and strength of the reconstructed NPJ during extreme wet/dry years in CA using a tree ring-based reconstruction of October$_{t-1}$-June$_t$ precipitation for the southern Sierra Nevada mountains (23), which is nearly independent of the NPJ reconstruction. In a similar way, we stratified NPJ winter conditions according to high- and low-fire years, as reconstructed from a completely independent record of Sierra Nevada fire history (24) (See SI Appendix, Fig. S2). We note that the annual precipitation at the fire record sites is generally similar to that in the precipitation reconstruction sub-region, which is included within the spatial extent of the fire record near its southern end (50). We also note that the spatial coverage of the extreme precipitation stratification in the 20CR v2 (Figs. 1e-f, 3a-d) is spatially as close to the independent Sierra Nevada paleo-precipitation record as possible, given the gridded nature of the reanalysis, and the 20CR v2 seasonal coverage also matches that of the Sierra Nevada record (October$_{t-1}$-June$_t$). Further methodological information is provided in the SI Appendix, *Additional Methodological Detail*.

Data Avaliability

The 200 hPa GPH and corresponding NPJ *u*- and *v*-wind reconstructions are housed upon publication with the World Data Service for Paleoclimatology, https://www.ncdc.noaa.gov/paleo-search/.

Acknowledgments

The authors thank J. Betancourt, S. Belmecheri, H. Diaz, C. Skinner, and E. Cook for fruitful discussions. The contribution by EZ is part of the German Science Foundation Cluster of Excellence Clisap (grant EXC177). EW's work was partially supported by Clisap. VT was supported by a US National Science Foundation CAREER grant (AGS-1349942) and a grant from the US Department of the Interior (USDI) Southwest Climate Science Center (US Geological Survey; G13AC00339). Support to AT and VT was provided by a cooperative agreement with the US Department of Agriculture (USDA) Forest Service (04-JV-11272162-407) with funds provided by the USDI/USDA Interagency Joint Fire Sciences Program, a George S. Deike Research Grant, and a Travel Grant from the Swiss National Science Foundation.

1 Bartos MD, Chester MV (2015) Impacts of climate change on electric power supply in the Western United States. *Nat Clim Change* 5:748-752.
2 Asner, GP et al. (2016) Progressive forest canopy water loss during the 2012-2015 California drought. *Proc Natl Acad Sci USA* 113:E249-E255.
3 Governor of California, https://www.gov.ca.gov/docs/4.7.17_Exec_Order_B-40-17.pdf.
4 Belmecheri S, Babst F, Wahl ER, Stahle DW, Trouet V (2016) Multi-century evaluation of Sierra Nevada snowpack. Nat Clim Change 6(1):2-3.
5 Los Angeles Times, http://www.latimes.com/local/lanow/la-me-ln-oroville-fema-payment-2-0170810-story.html.
6 CALFIRE. http://cdfdata.fire.ca.gov/incidents/incidents_stats?year=2017, accessed 1/10/2018.
7 Diffenbaugh NS, Swain DL, Touma D (2015) Anthropogenic warming has increased drought risk in California. *Proc Natl Acad Sci USA* 112:3931-3936.
8 Dettinger M (2011) Climate change, atmospheric rivers, and floods in California–a multi-model analysis of storm frequency and magnitude changes. *J Am Water Res Assoc* 47:514-523.
9 Abatzoglou JT, Balch JK, Bradley BA, Kolden CA (2018) Human-related ignitions concurrent with high winds promote large wildfires across the USA. *Int J Wildland Fire*, 27(6):377-386.
10 Pierce DW, *et al.* (2013) Probabilistic estimates of future changes in California temperature and precipitation using statistical and dynamical downscaling. *Clim Dyn* 40:839-856.
11 Swain DL, et al. (2014) The extraordinary California drought of 2013/2014: character, context, and the role of climate change. *Bull Am Met Soc* 95:S3-S7.
12 Funk C, Hoell A, Stone D (2014) Examining the contribution of the observed global warming trend to the California droughts of 2012/13 and 2013/14. *Bull Am Met Soc* 95:S11-S15.
13 Trouet V, Taylor AH, Carleton AM, Skinner CN (2009) Interannual variations in fire weather, fire extent, and synoptic-scale circulation patterns in northern California and Oregon. *Theor Appl Climatol* 95:349-360.
14 Trouet V, Taylor AH, Carleton A M, Skinner CN (2006) Fire-climate interactions in forests

of the American Pacific coast. *Geophys Res Lett* 33:L18704.
15 Diaz HF, Wahl ER (2015) Recent California Water Year Precipitation Deficits: A 440-Year Perspective. *J Clim* 28: 4637-4652.
16 Neiman PJ, Ralph FM, Wick GA, Lundquist JD, Dettinger MD (2008) Meteorological characteristics and overland precipitation impacts of atmospheric rivers affecting the West Coast of North America based on eight years of SSM/I satellite observations. *J Hydrometeor* 9:22-47.
17 Westerling AL (2016) Increasing western US forest wildfire activity: sensitivity to changes in the timing of spring. *Phil Trans R Soc B* 371:20150178.
18 Diaz H, Wahl E, Zorita E, Giambelluca T, Eischeid J (2016) A 480-year Reconstruction of Hawaiian Islands Rainfall. *J Clim* 29:5661-5674, doi:10.1175/JCLI-D-15-0815.1.
19 National Centers for Environmental Information, Climate at a Glance, https://www.ncdc.noaa.gov/cag/time-series/us.
20 Wahl E, Diaz H, Vose R, Gross W (2017) Multi-century evaluation of recovery from strong precipitation deficits in California. *J Clim* 30:6053-6063, doi:10.1175/JCLI-D-16-0423.1.
21 Wise E (2016) Five centuries of U.S. West Coast drought: Occurrence, spatial distribution, and associated atmospheric circulation patterns. *Geophys Res Lett* 43, doi:10.1002/2016GL0-68487.
22 Wise E, Dannenberg M (2014) Persistence of pressure patterns over North America and the North Pacific since AD 1500. *Nat Commun* 5:4912, doi:10.1038/ncomms5912.
23 Graumlich LJ (1993) A 1000-Year Record of Temperature and Precipitation in the Sierra Nevada. *Quat Res* 39:249-255.
24 Taylor AH, Trouet V, Skinner CN, Stephens S (2016) Socioecological transitions trigger fire regime shifts and modulate fire-climate interactions in the Sierra Nevada, USA, 1600-2015 CE. *Proc Natl Acad Sci USA* 113:13684-13689.
25 Hare S, Mantua N (2000) Empirical Evidence for North Pacific Regime Shifts in 1977 and 1989. *Prog Oceanogr* 47:103-145, doi:10.1016/S0079-6611(00)00033-1.
26 Compo GP, et al. (2011) The Twentieth Century Reanalysis Project. *Quart J Royal Meteorol Soc* 137:1-28.
27 Wise E, Dannenberg M (2017) Reconstructed storm tracks reveal three centuries of changing moisture delivery to North America. *Sci Adv* 3(6):e1602263.
28 Dannenberg M, Wise E (2017) Shifting Pacific storm tracks as stressors to ecosystems of western North America. *Glob Change Biol* 23:4896–4906, doi:10.1111/gcb.13748.
29 Swain D, Horton D, Singh D, Diffenbaugh N (2016) Trends in atmospheric patterns conducive to seasonal precipitation and temperature extremes in California. *Sci Adv* 2(4): e1501344.
30 Abatzogloua JT, Williams AP (2016) Impact of anthropogenic climate change on wildfire across western US forests. *Proc Natl Acad Sci USA* 113:11770–11775, doi:10.1073/pnas.160-7171113.
31 Chang EKM, Zheng C, Lanigan P, Yau AMW, Neelin JD (2015) Significant modulation of variability and projected change in California winter precipitation by extratropical cyclone activity. *Geophys Res Lett* 42:5983-5991.
32 Simpson IR, Seager R, Ting MF, Shaw, TA (2016) Causes of change in Northern Hemisphere winter meridional winds and regional hydroclimate. *Nature Clim Change* 6:65-70.
33 Ashfaq M, et al. (2013) Near-term acceleration of hydroclimatic change in the western US. *J Geophys Res Atmos* 118:10676-10693.
34 Huang X, Hall AD, Berg N (2018) Anthropogenic Warming Impacts on Today's Sierra Nevada Snowpack and Flood Risk. *Geophys Res Lett* 45, doi:10.1029/2018GL077432
35 Trouet V, Taylor AH, Wahl ER, Skinner CN, Stephens SL (2010) Fire-climate interactions in the American West since 1400 CE. *Geophys Res Lett* 37:L04702.
36 Adams MA (2013) Mega-fires, tipping points and ecosystem services: Managing forests and woodlands in an uncertain future. *For Ecol Manag* 294:250-261.
37 Dennison PE, Brewer SC, Arnold JD, Moritz MA (2014) Large wildfire trends in the western United States, 1984-2011. *Geophys. Res. Lett.* 41:2928-2933.
38 Liang S, Hurteau MD, Westerling AL (2017) Potential decline in carbon carrying capacity under projected climate-wildfire interactions in the Sierra Nevada. *Sci. Rep.* 7:art 2420.
39 Schenk F, Zorita E (2012) Reconstruction of high resolution atmospheric fields for Northern Europe using analog-upscaling. *Clim Past* 8:1681-1703.
40 Ohlwein C, Wahl ER (2012) Review of probabilistic pollen-climate transfer methods. *Quat Sci Rev* 31:17-29.
41 Wahl ER (2004) A general framework for determining cutoff values to select pollen analogs with dissimilarity metrics in the modern analog technique. *Rev Palaeobot Palyn* 128:263-280.
42 Gavin DG, Oswald WW, Wahl ER, Williams JW (2003) A statistical approach to evaluating distance metrics and analog assignments for pollen records. *Quat Res* 60:356-367.
43 Giorgetta MA, *et al.* (2013) Climate and carbon cycle changes from 1850 to 2100 in MPI-ESM simulations for the Coupled Model Intercomparison Project phase 5. *J Advanc Model Earth Syst* 5:572-597 (2013).
44 Landrum L, *et al.* (2013) Last Millennium Climate and Its Variability in CCSM4. *J Clim* 26:1085-1111.
45 Schmidt, GA, *et al.* (2014) Configuration and assessment of the GISS ModelE2 contributions to the CMIP5 archive. *J. Adv. Model. Earth Syst.*, 6:141–184, doi:10.1002/2013MS000265.
46 Cook ER, *et al.* (2010) Megadroughts in North America: placing IPCC projections of hydroclimatic change in a long-term palaeoclimate context. *J Quat Sci* 25:48-61.
47 Wahl ER, Diaz HF, Smerdon JE, Ammann CM (2014) Late winter temperature response to large tropical volcanic eruptions in temperate western North America: Relationship to ENSO phases. *Glob Plan Change* 122:238-250.
48 St George S, Meko DM, Cook ER (2010) The seasonality of precipitation signals embedded within the North American Drought Atlas. *Holocene* 20:983-988.
49 Graham NE, *et al.* (2007) Tropical Pacific – mid-latitude teleconnections in medieval times. *Clim Change* 83:241–285, doi:10.1007/s10584-007-9239-2.
50 Western Regional Climate Center, http://www.wrcc.dri.edu/C-limate/precip_map_show.php?simg=ca.png, 26 July, 2018
51 Ebisuzaki W (1997) A Method to Estimate the Statistical Significance of a Correlation When the Data Are Serially Correlated. *J. Clim.* 10:2147-2153, doi:10.1175/1520 0442(1997)010<2-147:AMTETS>2.0.CO;2.